A Transverse Tubule NADPH Oxidase Activity Stimulates Calcium Release from Isolated Triads via Ryanodine Receptor Type 1 S-Glutathionylation*

Cecilia Hidalgo[‡§1], **Gina Sánchez**[‡¶], **Genaro Barrientos**[‡], **and Paula Aracena-Parks**[‡2]

From the ‡*Centro FONDAP de Estudios Moleculares de la Célula, Facultad de Medicina,* §*Programa de Biología Celular y Molecular, Instituto de Ciencias Biomédicas, Facultad de Medicina, and* ¶*Programa de Patología, Instituto de Ciencias Biomédicas, Facultad de Medicina, Universidad de Chile, Casilla 70005, Santiago 7, Chile*

We report here the presence of an NADPH oxidase (NOX) activity both in intact and in isolated transverse tubules and in triads isolated from mammalian skeletal muscle, as established by immunochemical, enzymatic, and pharmacological criteria. Immunohistochemical determinations with NOX antibodies showed that the gp91^{phox} membrane subunit and the cytoplasmic regulatory p47^{phox} subunit co-localized in transverse tubules of adult mice fibers with the α_{1s} subunit of dihydropyridine receptors. Western blot analysis revealed that isolated triads contained the integral membrane subunits gp91^{phox} and p22^{phox}, which were markedly enriched in isolated transverse tubules but absent from junctional sarcoplasmic reticulum vesicles. Isolated triads and transverse tubules, but not junctional sarcoplasmic reticulum, also contained varying amounts of the cytoplasmic NOX regulatory subunits p47^{phox} and p67^{phox}. NADPH or NADH elicited superoxide anion and hydrogen peroxide generation by isolated triads; both activities were inhibited by NOX inhibitors but not by rotenone. NADH diminished the total thiol content of triads by one-third; catalase or apocynin, a NOX inhibitor, prevented this effect. NADPH enhanced the activity of ryanodine receptor type 1 (RyR1) in triads, measured through [^{3}H]ryanodine binding and calcium release kinetics, and increased significantly RyR1 S-glutathionylation over basal levels. Preincubation with reducing agents or NOX inhibitors abolished the enhancement of RyR1 activity produced by NADPH and prevented NADPH-induced RyR1 S-glutathionylation. We propose that reactive oxygen species generated by the transverse tubule NOX activate via redox modification the neighboring RyR1 Ca^{2+} release channels. Possible implications of this putative mechanism for skeletal muscle function are discussed.

The NADPH oxidases (NOX)[3] are flavoprotein enzymes that use NADPH as electron donor to mediate the univalent reduction of molecular oxygen to superoxide anion (1), a free radical that by spontaneous or enzymatically catalyzed dismutation is readily converted into H$_2$O$_2$. The phagocytic NOX isoform (NOX2) was first discovered as a pivotal component of the neutrophil respiratory burst (2, 3). The functional NOX2 enzyme is composed of two integral plasma membrane subunits, gp91^{phox} and p22^{phox}, which make up cytochrome b_{558}, plus three cytosolic regulatory subunits: p40^{phox}, p47^{phox}, and p67^{phox} (2, 4).

A variety of tissues, including endothelial cells (5), smooth muscle cells (6), neurons (7–9), and astrocytes (7, 10), possess nonphagocytic NOX homologues (11, 12). Several reports indicate that NOX2 and its homologues have a central role in the generation of reactive oxygen species (ROS) in response to diverse physiological extracellular stimuli (13–17). Moreover, membrane depolarization stimulates NOX activity in phagocytes (18) and endothelial cells (19, 20). NOX stimulation is also apparent following agonist-induced stimulation of N-methyl-D-aspartate receptors in hippocampal neurons (21). Some NOX isoforms, including NOX2, are also regulated by interaction with the small G protein Rac (2, 22). Regulation of the NOX4 isoform has been recently characterized as unusual among the NOX family, since this isoform displays constitutive activity (*i.e.* without relying on cytosolic components, such as Rac) and generates large amounts of hydrogen peroxide (23). The NOX5 isoform contains EF-hand motifs in its structure, a structural feature that makes it Ca^{2+}-dependent (24). Homologues of the p47^{phox} and p67^{phox} cytosolic components (NOXO1 and NOXA1), which selectively regulate NOX1 (25, 26) and NOX3 (27), have been also described.

Both the NOX2 and the NOX4 isoforms are present in cardiac muscle cells (28). NADPH addition to microsomes isolated from heart muscle significantly enhances, via NOX activation, both RyR2 S-glutathionylation and Ca^{2+}-induced Ca^{2+} release (CICR) (29). Skeletal muscle homogenates also contain all of the NOX2 protein components and display an activity that generates superoxide anion at the expense of NADH oxidation

[3] The abbreviations used are: NOX, NADPH oxidase; BSA, bovine serum albumin; CICR, Ca^{2+}-induced Ca^{2+} release; DHPR, dihydropyridine receptor(s); DPI, diphenyleneiodonium; E-C, excitation-contraction; RyR1, ryanodine receptor type 1; ROS, reactive oxygen species; PBS, phosphate-buffered saline; SH, sulfhydryl; SOD, superoxide dismutase; SR, sarcoplasmic reticulum; T-tubule, transverse tubule; MOPS, 4-morpholinepropanesulfonic acid.

(30). In addition, human skeletal muscle tissue exhibits transcripts for the NOX2 and NOX4 isoforms (31). All of these findings provide experimental support to earlier proposals suggesting the presence of NOX in skeletal muscle cells (32, 33). We have found recently that tetanic field stimulation of rat skeletal muscle cells in primary culture increases NOX-dependent ROS production and elicits ryanodine-sensitive Ca^{2+} signals that are significantly decreased by NOX inhibitors.[4] These results suggest a role for activity-dependent NOX as a source of RyR-modifying ROS in skeletal muscle.

In this work, we investigated the membrane origin of the skeletal muscle NOX and the effects of NOX-generated ROS on RyR1 activity and RyR1 *S*-glutathionylation levels. For these experiments, we used either intact fibers isolated from adult mouse skeletal muscle or three different membrane fractions isolated from rabbit skeletal muscle: transverse tubules (T-tubules), triads (which contain 10–15% T-tubules attached to junctional sarcoplasmic reticulum (SR) vesicles), and junctional (heavy) SR vesicles devoid of T-tubules but enriched in RyR1 channels. Immunohistochemistry with specific antibodies showed that the NOX membrane gp91^{phox} subunit and the cytoplasmic p47^{phox} regulatory subunit co-localized with the α_{1s} subunit of dihydropyridine receptors (DHPR) in T-tubules of adult mice fibers. Western blot analysis showed that the NOX integral membrane components gp91^{phox} and p22^{phox} were markedly enriched in T-tubules and also present in triads but were absent from heavy SR vesicles. Triads displayed NADPH-dependent generation of superoxide anion and H_2O_2 that was significantly decreased by NOX inhibitors. In addition to promoting NOX activity, NADPH enhanced significantly RyR1 *S*-glutathionylation and increased RyR1 activity. Possible physiological consequences of these findings, in terms of potential cross-talk between redox and calcium signaling cascades that may lead to enhanced Ca^{2+} release in skeletal muscle, are discussed.

EXPERIMENTAL PROCEDURES

Materials—All reagents used were of analytical grade. Ryanodine, bovine serum albumin, bovine liver catalase, β-mercaptoethanol, and protease inhibitors (leupeptin, pepstatin A, benzamidine, and phenylmethylsulfonyl fluoride) were from Sigma. Bovine erythrocyte superoxide dismutase (SOD), rotenone, NADH, NADPH, lucigenin, 2,4-dithiothreitol, diphenyleneiodonium (DPI), 5,5′-dithiobis-(2-nitrobenzoic) acid, and N^G-nitro-L-arginine methyl ester were from Calbiochem. [^{3}H]Ryanodine was from PerkinElmer Life Sciences, apocynin was from Aldrich, and 10-acetyl-3,7-dihydrophenoxazine (Amplex Red reagent) was from Molecular Probes, Inc. (Eugene, OR). Polyvinylidene difluoride membranes were from Bio-Rad.

Antibodies—The mouse monoclonal anti-gp91^{phox}, anti-p22^{phox}, anti-p47^{phox}, and anti-p67^{phox} antibodies used for Western blot assays were a kind gift from Dr. Mark T. Quinn (Veterinary Molecular Biology, Montana State University, Bozeman, MT); these antibodies were raised as described previously (34). The goat polyclonal anti-gp91^{phox} and anti-p47^{phox}

antibodies used for immunohistochemical experiments, as well as the antibodies against RyR or horseradish peroxidase-conjugated anti-IgG (anti-mouse or anti-rabbit) were from Santa Cruz Biotechnology, Inc. (Santa Cruz, CA). The anti-glutathione (anti-GSH) antibody was from Virogen (Watertown, MA). Mouse monoclonal antibodies against the α_{1s} subunit of DHPR were from Affinity BioReagents (Golden, CO), and Alexa Fluor secondary antibodies were from Molecular Probes.

Fiber Isolation and Immunohistochemistry—Adult AJ mice were anesthetized with ketamine, following a procedure approved by the local animal ethics committee. The flexor digitorum longus or tibialis anterioris muscles were dissected out, placed in Krebs solution (135 mM NaCl, 5.9 mM KCl, 1.2 mM $MgCl_2$, 1.5 mM $CaCl_2$, 11.5 mM Hepes, pH 7.4, 11.5 mM glucose) and immediately fixed in 4% paraformaldehyde in PBS (134 mM NaCl, 2.7 mM KCl, 17 mM Na_2HPO_4, 2.3 mM KH_2PO_4, pH 7.4) for 30 min at room temperature. After three washes with PBS, muscle fibers were obtained by gentle mechanical dissociation with a surgical tool. Isolated fibers were permeabilized with 0.05% Triton X-100 added to PBS containing 1% bovine serum albumin (BSA) to block nonspecific binding sites. After a 10-h incubation, the Triton X-100 solution was replaced by PBS plus 1% BSA; antibodies against gp91^{phox}, p47^{phox}, or the α_{1s} subunit of DHPR were added at a 1:100 dilution; and the fibers were incubated for 10 h at room temperature. Fibers were washed three times with PBS plus 1% BSA and were incubated for 1 h with Alexa Fluor secondary antibodies (1:500). After five washes with PBS plus 1% BSA, fibers were placed on glass coverslips to record fluorescent images in an inverted confocal microscope (Carl Zeiss LSM 5 Pascal, Oberkochen, Germany). Fluorescent images were analyzed with the Image J 1.32j software; the percentage of colocalization was estimated using the colocalization finder plugin, version 1.1. Control experiments with the secondary antibodies did not show detectable fluorescence.

Membrane Isolation—Membrane preparations from rabbit fast skeletal muscle were isolated as described previously (35, 36). Triad-enriched SR vesicles isolated from rabbit muscle (hereafter referred to as triads) contain 10–15% attached T-tubules, as evidenced by their density of [^{3}H]ouabain binding sites. Membrane fractions were stored in liquid nitrogen and were used within 3 days; longer storage resulted in significant deterioration of NOX activity. Protein was determined (37) using commercial BSA as a standard.

Western Blotting—Triad vesicles (10 μg) were incubated in nonreducing loading buffer (6 M urea, 1% SDS, 0.02% bromphenol blue, 50 mM NaH_2PO_4, 17 mM Na_2HPO_4) plus 5 mM *N*-ethylmaleimide at 60 °C for 20 min. Proteins were separated in 3.5–8% gradient gels by SDS-PAGE under nonreducing conditions, as described elsewhere (38). For RyR1 detection, proteins were transferred to polyvinylidene difluoride membranes at 350 mA for 3 h at 4 °C; for smaller molecular weight proteins, the transfer times were only 1 h under the same conditions. Membranes were blocked with 5% BSA in Tris-saline buffer (140 mM NaCl, 20 mM Tris-HCl, pH 7.6) plus 0.2% Tween 20 and were probed with specific antibodies directed to RyR, GSH, gp91^{phox}, p22^{phox}, p47^{phox}, or p67^{phox}. Horseradish peroxidase-conjugated anti-mouse or anti-rabbit IgG was used as second-

ary antibody. Blots were developed using an ECL kit (Pierce). Membranes were stripped between blots by 30-min incubation at 50 °C with a solution containing 100 mM β-mercaptoethanol, 2% SDS, 62.5 mM Tris-HCl, pH 6.7.

Determination of NADPH Oxidase Activity—To determine NOX activity, we measured the oxidation of both NADH and NADPH as well as the generation of superoxide anion and H_2O_2. Oxidation of NADH or NADPH by triads (0.1 mg/ml) was monitored at 340 nm ($\epsilon = 6,250$ M^{-1} cm^{-1}) in a Hewlett-Packard ChemStation UV-visible spectrophotometer (Waldbronn, Germany). Superoxide generation was measured by the lucigenin-derived chemiluminiscence method in a Berthold FB 12 luminometer; SR vesicles (0.2 mg/ml) were incubated at 25 °C with 100 mM MOPS-Tris, pH 7.0, 5 μM lucigenin, and variable concentrations of NADPH, as specified in each case. Chemiluminiscence was expressed as nmol of superoxide ion generated/mg of protein/min; calibration was done using hypoxanthine and xanthine oxidase as described (30). Hydrogen peroxide generation was measured at 37 °C or at 25 °C in a FluoroMax 2 spectrofluorotometer (ISA Jobinybon-Spex) with $\lambda_{ex} = 527$ nm, $\lambda_{em} = 583$ nm, using Amplex Red as described (39). The effects of DPI (10 μM), apocynin (4 mM), rotenone (200 nM), N^G-nitro-L-arginine methyl ester (2 mM), and SOD (300 units/ml) on superoxide anion or H_2O_2 generation were also tested, as indicated in each case. Nonenzymatic controls were performed using vesicles heat-denatured for 10 min at 100 °C; this procedure essentially abolished H_2O_2 generation and reduced by >90% NADH/NADPH oxidation and superoxide anion generation. To calculate specific activities, the activity displayed by heat-denatured vesicles was subtracted from the total activity.

Detection of Endogenous or NADPH-promoted RyR1 S-Glutathionylation—To detect endogenous RyR1 S-glutathionylation, triad vesicles (10 μg) were separated by SDS-PAGE under nonreducing conditions as described above. After electrophoresis and transfer to polyvinylidene difluoride membranes, proteins were probed with anti-GSH antibody (1:10,000). Following ECL detection of the antigen-antibody reaction, membranes were stripped and probed with anti-RyR antibody. Blots were quantified by densitometric analysis (Quantity One software; Bio-Rad). Results were expressed as the ratio of anti-GSH/anti-RyR band densities. To detect NADPH-promoted S-glutathionylation, triad vesicles (1 mg/ml) were incubated at 25 °C for 10 min in a solution containing 0.1–0.5 mM NADPH, 100 mM MOPS-Tris, pH 7.0. The effect of apocynin (8 mM) was tested in some experiments.

Labeling of Triad Proteins with [^{35}S]GSH—Vesicles were incubated for 10 min at 37 °C in a solution containing 100 mM MOPS-Tris, pH 7.2, 0.1 mM NADPH plus [^{35}S]GSH added as tracer. The reaction was terminated by the addition of nonreducing sample buffer plus 5 mM N-ethylmaleimide. Triad proteins (10 μg) were separated in 3.5–8% nonreducing gels as above. Gels were stained with Coomassie Blue, and the ^{35}S radioactivity incorporated into RyR1 was determined in a Molecular Imager FX system (Bio-Rad) using a CP Phosphor Screen (Eastman Kodak Co.) essentially as reported earlier (38).

Titration of Total Sulfhydryl Content—Triads were incubated at 0.1 mg/ml at 37 °C for 10 min with or without 0.1 mM

NADH; samples were taken at different times to determine their total sulfhydryl content. For this purpose, triads were incubated for an additional 30-min period at 25 °C with 0.1 mM 5,5′-dithiobis-(2-nitrobenzoic) acid in 50 mM Tris-base (40). Alternatively, triads (0.1 mg/ml) were incubated with 100 μM H_2O_2 for 10 min at 37 °C prior to sulfhydryl titration as above. The effects of apocynin (2 mM) or catalase (300 units/ml) were tested in some experiments.

Detection of NADPH-dependent S–S Cross-link Formation between RyR1 Subunits—Triads were incubated for 10 min at 37 °C with 0.1 mM NADPH or with 0.25 mM diamide. To analyze RyR cross-linked products, the procedure described in detail elsewhere (41) was followed without substantial modifications.

[^{3}H]Ryanodine Binding—To measure initial rates of [^{3}H]ryanodine binding, triads (0.2 mg/ml) were incubated at pCa 5 under high ionic strength conditions (500 mM KCl, 20 mM MOPS-Tris, pH 7.2). Total binding, determined in the presence of 5 nM [^{3}H]ryanodine, was measured at 37 °C for 10 min, taking samples at 5-, 7-, and 10-min intervals; nonspecific binding was determined in the additional presence of 10 μM ryanodine. To test the effects of NADH, NADPH, GSH, or DPI, vesicles were preincubated with these reagents for 2 min at 25 °C. The effects of SOD plus catalase or of H_2O_2 were tested in some experiments.

Calcium Release Kinetics—Calcium release kinetics was determined as described in detail elsewhere (38). Briefly, triads were actively loaded with calcium by incubation for 10 min at 25 °C in a solution containing 100 mM KCl, 2 mM ATP (sodium salt), 3 mM $MgCl_2$, 20 mM MOPS/Tris, pH 7.20, 10 mM phosphocreatine, and 15 units/ml creatine kinase. Vesicles were then mixed (1:10) in a stopped flow fluorescence spectrophotometer with a releasing solution containing 100 mM KCl, 7 mM ATP-Na, 5.56 mM $MgCl_2$, 0.165 mM $CaCl_2$, 20 mM MOPS/Tris, pH 7.20, plus 1 μM Calcium Green-5N. Upon mixing, free concentrations were 1.4 mM ATP, 0.348 mM Mg^{2+}, and 0.019 mM Ca^{2+} (pCa 4.7). To test the effects of NADPH, GSH, or DPI on calcium release kinetics, vesicles were incubated with these reagents for 10 min at 25 °C during active loading as above.

Statistical Analysis—Data are presented as mean ± S.E. of at least three independent determinations. For statistical comparisons, depending on the number of determinations, an analysis of variance test was performed either with Dunnett post-test analysis using the GraphPad® Prism software or the Holm-t test using the Primer of Bioestatistics software. Values were considered significantly different if p was <0.05.

RESULTS

Occurrence of NADPH Oxidase Subunits in Transverse Tubules of Mouse Skeletal Muscle Fibers—Rat skeletal muscle contains mRNA and proteins for the NOX gp91^{phox}, p22^{phox}, p47^{phox}, and p67^{phox} subunits localized in close proximity to the sarcolemma, albeit their precise membrane location was not specified (30). Our earlier observations[5] indicating that isolated T-tubules but not SR vesicles oxidized NADH at high rates suggested a T-tubular location for this NADH oxidase activity.

---

[5] J. L. Fernandez and C. Hidalgo, unpublished observations.

α₁ₛ DHPR   gp91ᵖʰᵒˣ

Transmitted   Merged

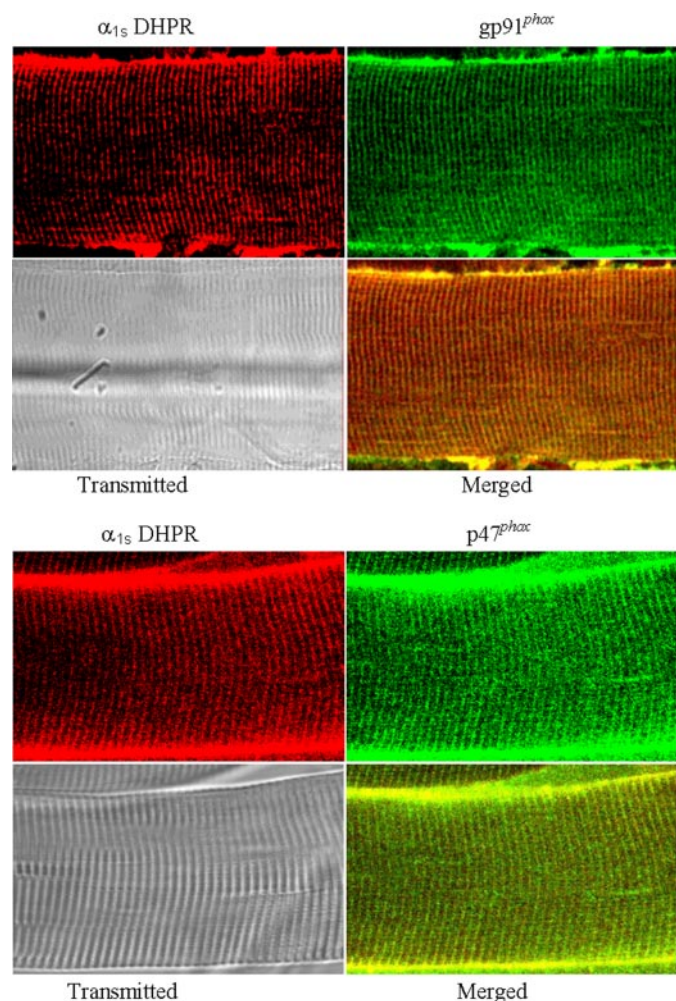α₁ₛ DHPR   p47ᵖʰᵒˣ

Transmitted   Merged

FIGURE 1. **Immunohistochemistry of fibers dissociated from adult mouse skeletal muscle.** The *top panel* illustrates the pattern obtained with α1-DHPR and gp91ᵖʰᵒˣ antibodies, and the *bottom panel* illustrates the pattern obtained with α1-DHPR and p47ᵖʰᵒˣ antibodies; in both cases, the transmitted image of the fiber and the co-localization (in *yellow*) are also shown. Secondary antibodies conjugated with Alexa 488 or Alexa 633 for α1-DHPR (*green*) or the NOX subunits (*red*), respectively, were used. For further details, see "Experimental Procedures."

In this work, we detected the presence of the NOX subunits gp91ᵖʰᵒˣ and p47ᵖʰᵒˣ in skeletal muscle fibers from adult mice (Fig. 1). Over 95% colocalization of these two NOX subunits with the α_{1S} DHPR subunit was found in confocal serial images, strongly suggesting that the skeletal muscle NOX is localized in the T-tubule system.

Presence of NOX Protein Subunits in Isolated Triads and T-tubule Vesicles—Western blot analysis of isolated triads, T-tubules, and heavy SR vesicles revealed that antibodies against the NOX integral membrane subunit gp91ᵖʰᵒˣ or p22ᵖʰᵒˣ recognized protein bands in triads but not in heavy SR vesicles; these two protein bands were markedly enriched in isolated T-tubules (Fig. 2). The enrichment in gp91ᵖʰᵒˣ and p22ᵖʰᵒˣ in T-tubules relative to triads was consistently observed in all preparations studied. Antibodies against the NOX cytosolic components p47ᵖʰᵒˣ and p67ᵖʰᵒˣ also recognized protein bands in T-tubules and triads but not in heavy SR vesicles (Fig. 2). In contrast to the bands recognized by antibodies against gp91ᵖʰᵒˣ and p22ᵖʰᵒˣ, these two regulatory components were
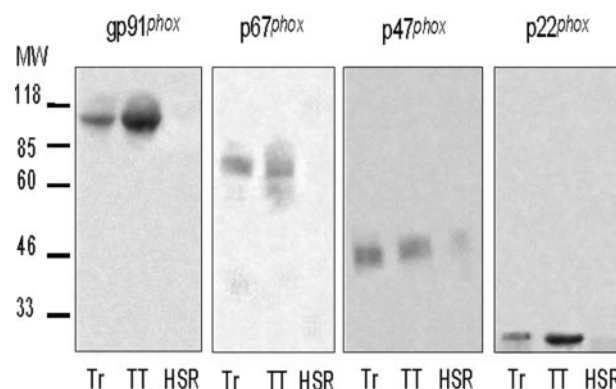

FIGURE 2. **Immunolocalization of the NADPH oxidase subunits in triads and T-tubule vesicles.** Triads (*Tr*), T-tubule (*TT*), and heavy SR vesicles (50 μg of total protein each) were subjected to Western blot analysis with the NOX antibodies indicated in the figure, as detailed under "Experimental Procedures." Blots are representative of three independent experiments. *MW*, molecular weight.

not enriched in the isolated T-tubule preparation illustrated in Fig. 2. Furthermore, some isolated T-tubule preparations had somewhat lower p47ᵖʰᵒˣ and p67ᵖʰᵒˣ contents than triads, suggesting that these regulatory subunits were lost to varying degrees during T-tubule isolation. This finding may explain why our attempts to measure NADH/NADPH oxidation and the coupled ROS generation by isolated T-tubule vesicles yielded variable results (see below).

The presence of the two NOX integral subunits gp91ᵖʰᵒˣ and p22ᵖʰᵒˣ in triads but not in heavy SR vesicles plus their marked enrichment in T-tubules reinforce the proposal that the skeletal NOX enzyme is a T-tubule enzyme.

NADPH Oxidase Activity in Triads—As described below, isolated triad vesicles, which are composed by junctional T-tubule and SR membranes, contain a NOX activity that can oxidize both NADH- and NADPH-generating superoxide anion and H₂O₂. Isolated triads have the capacity to promote significant oxidation of 0.1 mM NADPH or NADH, as illustrated in Fig. 3*A*. On average, at 37 °C, triads oxidized NADPH at a rate of 25.1 ± 1.4 nmol/mg/min ($n = 3$) and NADH at a rate of 20.5 ± 1.3 nmol/mg/min ($n = 7$). Lowering the reaction temperature to 25 °C decreased NADPH oxidation to 14 ± 1.2 nmol/mg/min ($n = 3$).

The addition to triads of increasing NADPH concentrations, from 100 μM to 1 mM, immediately elicited superoxide anion generation; at 25 °C, the reaction followed a linear time course for up to 20 min (Fig. 3*B*, *left*), and at 100 μM NADPH, the average rate was 2.01 ± 0.12 nmol/mg/min ($n = 10$). Increasing [NADPH] to 1 mM produced a hyperbolic increase in the rate of superoxide anion generation, with an apparent K_m of 204 ± 49 μM and a V_{max} of 6.25 ± 0.06 nmol/mg/min. The addition of 10 μM DPI or SOD (300 units/ml) inhibited markedly the rate of superoxide anion generation induced by 100 μM NADPH; 4 mM apocynin exerted a less pronounced inhibitory effect, whereas rotenone (200 nM) had no effect (Fig. 3*B*, *right*). Preincubation with 2 mM N^G-nitro-L-arginine methyl ester, a nitric-oxide synthase inhibitor, did not produce detectable effects on superoxide anion generation (data not shown). These results make unlikely mitochondrial contribution or nitric-oxide synthase as sources of superoxide anion.
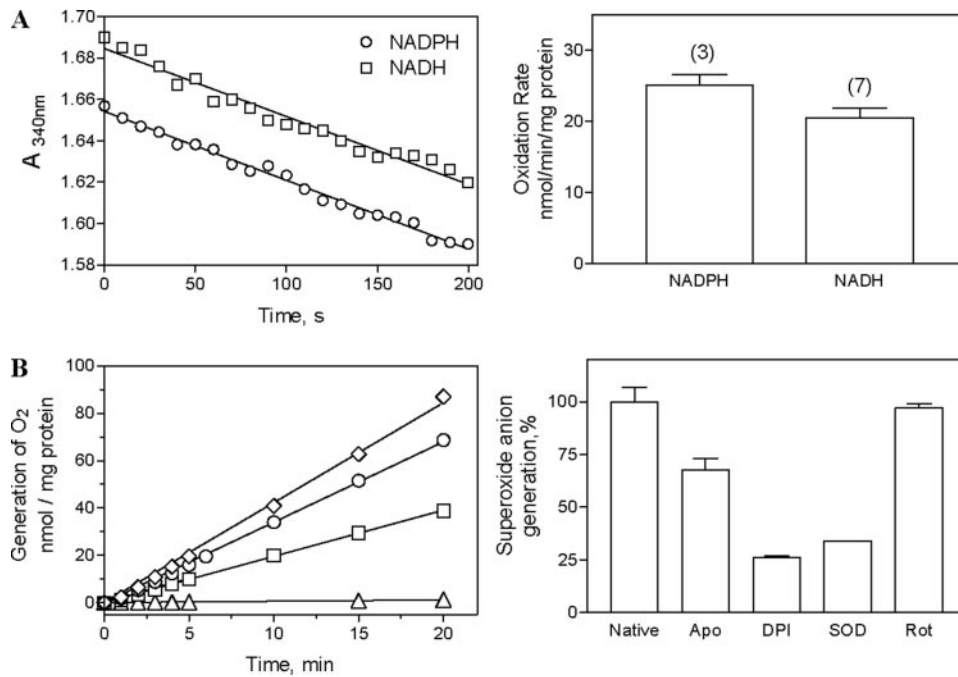
FIGURE 3. **Determination of NADPH oxidase activity in isolated triad vesicles.** *A*, the *left panel* shows the time course of oxidation of 0.1 mM NADPH (*open circles*) or 0.1 mM NADH (*open squares*). The *right panel* illustrates the corresponding average rates of oxidation; *numbers above* the *bars* indicate the number of determinations. *B*, the *left panel* shows the time course of superoxide anion generation following the addition of variable NADPH concentrations: 0 (*open triangles*), 0.1 mM (*open squares*), 0.5 mM (*open circles*), or 1.0 mM NADPH (*open diamonds*). The *right panel* illustrates the effects of apocynin (*Apo*), DPI, SOD, or rotenone (*Rot*) on the rate of superoxide anion generation elicited by 0.1 mM NADPH, expressed as percentage of control values. Further details are provided under "Experimental Procedures."
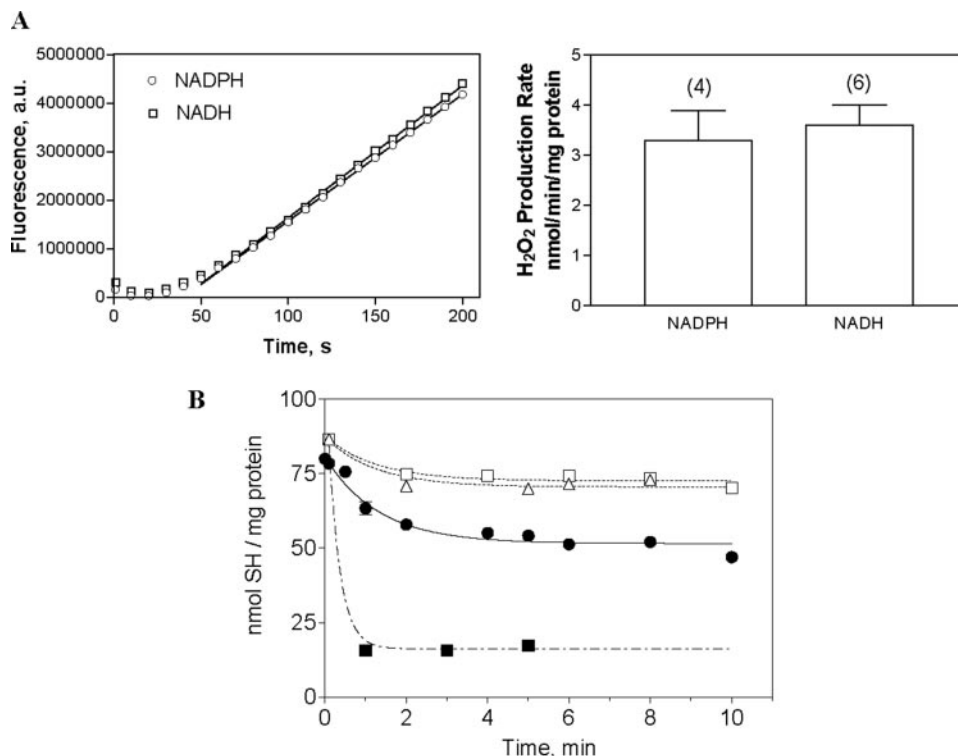

FIGURE 4. **Generation of hydrogen peroxide induced by NADPH or NADH (*A*) and effects of different agents on the free sulfhydryl content of triads (*B*).** *A*, the *left panel* shows the time course of H_2O_2 generation by 0.1 mM NADPH (*open circles*) or 0.1 mM NADH (*open squares*). The *right panel* illustrates the corresponding average rates of H_2O_2 generation; the *numbers above* the *bars* indicate the number of determinations. *B*, the total free sulfhydryl content of triads was determined as a function of time following the addition of 0.1 mM H_2O_2 (*solid squares*), 0.1 mM NADH (*solid circles*), 2 mM apocynin (*open triangles*), or 300 units/ml catalase (*open squares*). For details, see "Experimental Procedures."

The addition of 0.1 mM NADPH or NADH to triad vesicles induced H_2O_2 generation after a short delay (Fig. 4*A*, *left*). The average H_2O_2-generating activities at 37 °C (calculated from the linear part of the curves) were 3.3 ± 0.6 ($n = 4$) and 3.6 ± 0.4 ($n = 6$) (in nmol/mg/min) for triads incubated with 0.1 mM NADPH or NADH, respectively (Fig. 4*A*, *right*). At 25 °C, triads incubated with 0.1 mM NADPH generated 1.18 nmol of H_2O_2/mg of protein/min; the addition of 4 mM apocynin decreased this rate to 0.39 nmol of H_2O_2/mg of protein/min.

The presence of the regulatory cytosolic NOX components in triads (Fig. 2) indicates that these vesicles retain these subunits after isolation. This feature presumably explains why we could detect significant NOX activity in isolated triads, which always displayed comparable values of NADPH-dependent ROS generation. In contrast, some isolated T-tubule preparations displayed high DPI-sensitive activity, whereas others displayed activities lower than the NOX activity of triads.

In summary, these combined results strongly suggest that their T-tubule component endows triads with the ability to oxidize both NADH and NADPH, generating superoxide anion and hydrogen peroxide. Assuming a theoretical stoichiometry of 2 mol of superoxide anion produced per mol of NADPH oxidized, only a fraction (about 8%) of the total NADPH oxidative activity of triads measured with 0.1 mM NADPH seems to be coupled to superoxide anion generation. Presumably, triads possess other activities unrelated to NOX that can also oxidize NADH or NADPH (see "Discussion"). In contrast, a ratio of 1.7 was obtained at 25 °C between the rates of superoxide anion and H_2O_2 generation, suggesting that H_2O_2 generation by triads is tightly coupled to NOX-dependent superoxide anion production.

Oxidative Effects of Triad-associated NOX Activity—We studied next if the oxidative products generated by triadic NOX activity

decreased the total free sulfhydryl (SH) content of triads. As illustrated in Fig. 4*B*, at 37 °C, the addition of NADH (0.1 mM) to triads decreased in about 4 min their total SH content, from 85 to 51 nmol/mg of protein; this decrease was almost completely prevented by apocynin (2 mM) or catalase (300 units/ml). For comparison, the addition of 0.1 mM H_2O_2 diminished within 1 min the total triadic SH content to 16 nmol/mg of protein (80% decrease). These results suggest that NOX-generated ROS share with H_2O_2 the ability to readily remove free SH residues from triad proteins.

Triad-associated NOX Induced Stimulation of RyR1 Activity—We studied next if the stimulation of NOX by NADPH in triads can modify RyR1 activity through ROS-induced activation. To measure RyR1 activity, we determined [3H]ryanodine binding rates or the kinetics of RyR1-mediated CICR from triads.

Incubation of triads with either 0.1 mM NADPH or NADH produced a significant increase in [3H]ryanodine binding rates over controls (Fig. 5*A*), indicating increased RyR1 activity. In contrast, the addition of 0.2 mM GSH did not modify [3H]ryanodine binding rates when added to control vesicles but prevented the stimulation induced by 0.1 mM NADPH, as did DPI (10 μM) (Fig. 5*A*). Apocynin (4 mM), which by itself induced a 2-fold increase in [3H]ryanodine binding rates, prevented completely the stimulation induced by 0.1 mM NADH (data not shown). These results suggest that RyR1 stimulation by NADPH was NOX-mediated. Consistent with previous reports (42), we also found that H_2O_2 enhanced RyR1 activity (Fig. 5*B*). The stimulatory effect of H_2O_2, as revealed by the increase of [3H]ryanodine binding rates, was concentration-dependent, with a $K_{0.5}$ value of 2.7 μM (Fig. 5*C*). Catalase, which by itself did not affect [3H]ryanodine binding rates, significantly prevented this stimulation (Fig. 5*B*).

In isolated skeletal SR vesicles, stimulation of [3H]ryanodine binding by 1 mM NADPH has been reported (43). We found that increasing NADH from 0.1 to 1 mM produced a further increment in [3H]ryanodine binding to triads. However, as reported previously (43), DPI failed to inhibit the stimulation induced by 1 mM NADH (data not shown), suggesting that this effect is not NOX-mediated.

We have shown previously that redox modification of RyR1 channels, in particular *S*-glutathionylation, allows CICR in the presence of free Mg^{2+} concentrations that suppress endogenous RyR1 activity (38). Accordingly, we measured the effects of H_2O_2 and NADPH on CICR kinetics in the presence of 0.35 mM free $[Mg^{2+}]$, a condition that significantly inhibits CICR in native vesicles. The kinetics of CICR in native vesicles followed a double exponential function (Fig. 6*A*), with rate constants k_1 and k_2; the faster exponential, with $k_1 = 3.2$ s^{-1}, represented 42–45% of the total release. The addition of H_2O_2 produced a significant stimulation of CICR kinetics, as illustrated in Fig. 6*A*, increasing k_1 to 31.5 s^{-1}. As shown in Fig. 6*B*, 0.25 mM NADPH plus 50 μM GSH also induced a significant stimulation of CICR kinetics over the control and increased k_1 from 3.8 to 8.8 s^{-1}. In the absence of NADPH, 50 μM GSH did not affect k_1, which was 4 s^{-1}, but significantly decreased the magnitude of the second exponential. Varying [NADPH] from 0.1 mM to 0.25 or 0.5 mM in the constant presence of 50 μM GSH produced a
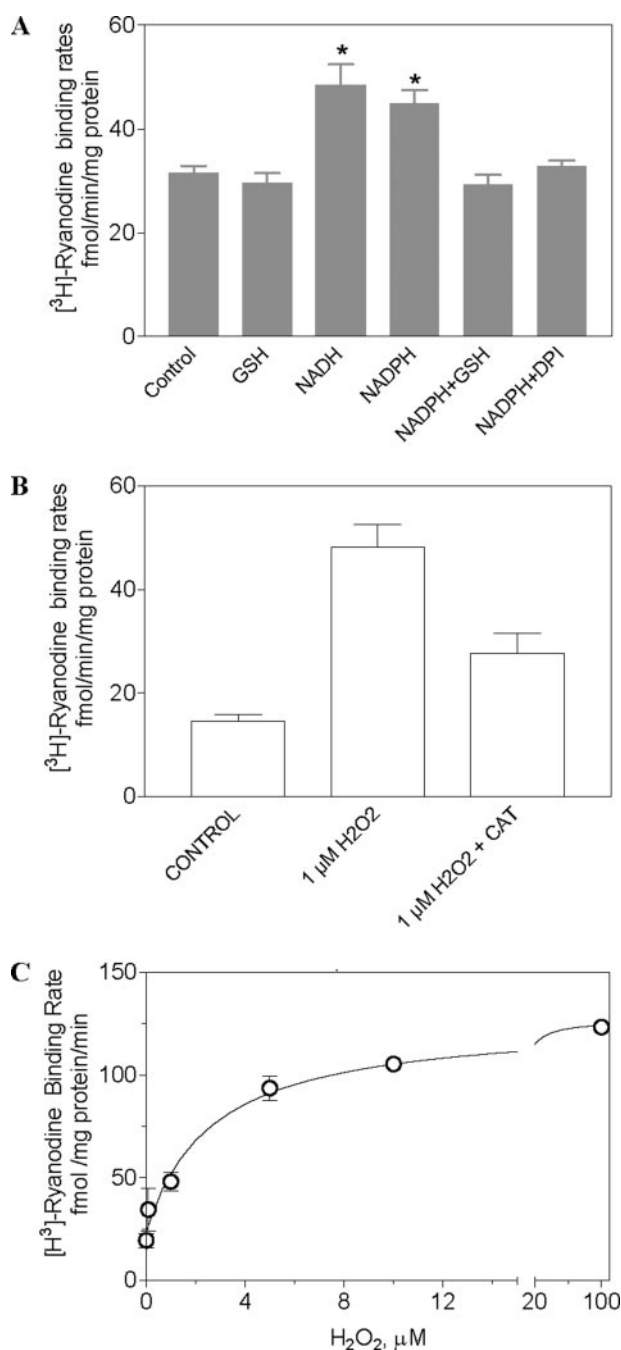

FIGURE 5. **[3H]ryanodine binding rates to isolated triad vesicles.** *A*, data were obtained after incubation of vesicles with 0.2 mM GSH, 0.1 mM NADH, 0.1 mM NADPH, 0.2 mM GSH + 0.1 mM NADPH, or 0.1 mM NADPH + 10 μM DPI. *B*, data were obtained after incubation of vesicles with the concentrations of H_2O_2 indicated in the figure. *C*, effect of increasing H_2O_2 concentration on the rates of [3H]ryanodine binding. Nonlinear fit of these data yielded a $K_{0.5}$ value of 2.7 μM. See "Experimental Procedures" for further details.

similar increase in k_1, as illustrated in Fig. 6*C*. These results suggest that 0.1 mM NADPH induced maximal stimulation of CICR. The CICR kinetics enhancement produced by 0.1 mM NADPH was inhibited by 10 μM DPI (not shown), suggesting strongly that the stimulation of CICR produced by NADPH was NOX-mediated.

Triad-associated NOX Enhanced RyR1 S-Glutathionylation—To test if the enhanced RyR1 activity produced by NADPH was due to specific redox modification of the RyR1
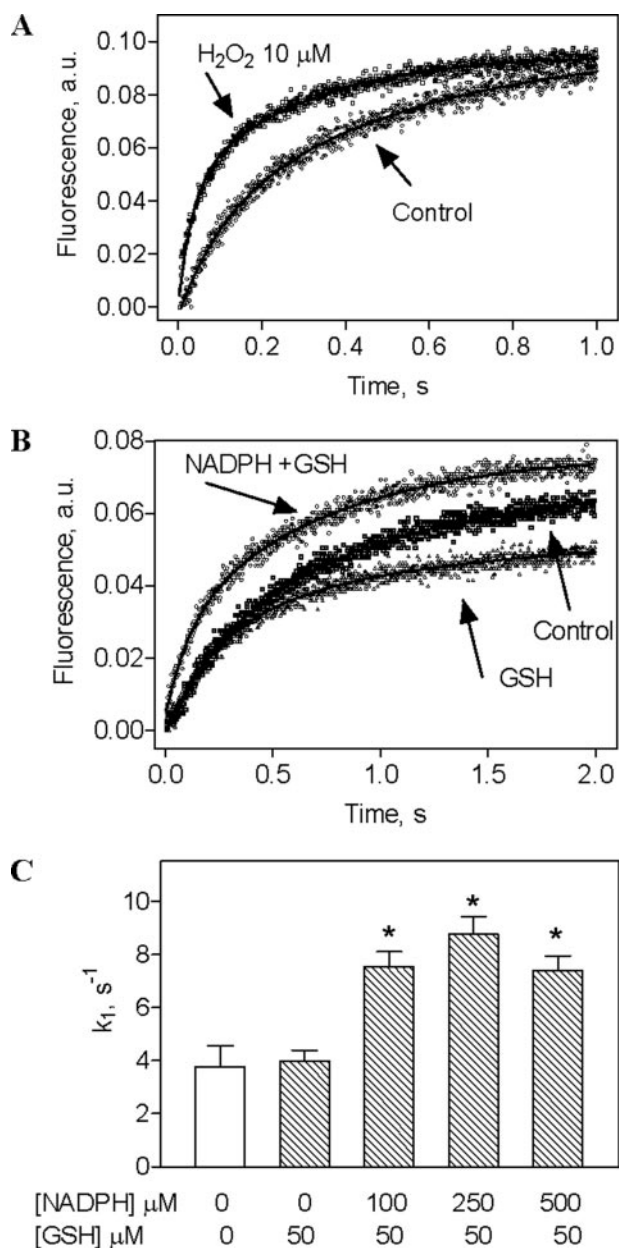
FIGURE 6. **Fast kinetics of CICR determined in isolated triad vesicles.** *A*, the kinetics of CICR, measured at high free $[Mg^{2+}]$ as detailed under "Experimental Procedures," was determined in native vesicles (control) or in vesicles preincubated with 10 μM H_2O_2. *B*, CICR kinetics, measured as above, was determined in native vesicles (control) or in vesicles preincubated with 50 μM GSH or with 0.25 mM NADPH plus 50 μM GSH. *C*, the values of the rate constant k_1, calculated from traces of CICR kinetics measured as above, are given for native vesicles or after the addition of varying [NADPH] plus 50 μM GSH. For further details, see "Experimental Procedures."

protein, we measured the *S*-glutathionylation levels displayed by RyR1 in control triads or after incubation for 10 min at 25 °C with NADPH. As illustrated in Fig. 7*A*, 0.1 mM NADPH enhanced significantly RyR1 *S*-glutathionylation 1.7-fold over the endogenous levels; apocynin (8 mM) prevented this increase. In the same conditions, incubation with 50 μM GSH plus 100 μM NADPH produced an even higher increase in RyR1 *S*-glutathionylation (2.8-fold), whereas increasing NADPH to 250 or 500 μM did not produce additional marked stimulation (Fig. 7*B*). These results show that both the stimulation of CICR

kinetics and of RyR1 *S*-glutathionylation was close to maximal at 0.1 mM NADPH.

We explored, in addition, if incubation of triads with [35S]GSH promoted the covalent incorporation of 35S into RyR1. As shown in Fig. 7*C*, significant 35S incorporation into RyR1 was detected when triads were incubated with 0.1 mM NADPH, an unequivocal demonstration of RyR1 *S*-glutathionylation; the presence of 2,4-dithiothreitol during incubation with NADPH prevented this RyR1 redox modification.

We also investigated if NADPH could also induce RyR1 cross-linking through S–S bond formation, a redox modification known to enhance RyR1 activity (41). Whereas incubation with diamide induced dimer formation as reported (41), no detectable formation of RyR1 dimers or higher molecular weight species was apparent following incubation of triads with 0.1 mM NADPH for 10 min at 37 °C (data not shown).

DISCUSSION

A growing body of evidence indicates that a transient increase of intracellular ROS is essential for cell signaling and regulation (44, 45). Diverse extracellular physiological stimuli promote the generation of ROS that have an effect on signaling pathways (14, 17, 46). In particular, H_2O_2 plays an important role in the regulation of cell signaling events (14, 47, 48), including control of gene expression (49, 50) and regulation of signal transduction cascades (51). Physiological regulation of cell signaling events by ROS occurs primarily via selective modification of cysteine residues within proteins. Since cells possess specific systems to reverse these protein redox modifications (52, 53), transient modifications of cysteine residues are likely to be central to the mechanisms underlying redox regulation of normal cell function (54, 55).

Skeletal muscle generates ROS following contraction (56, 57) and during heat stress conditions (58), and the presence of a ROS-generating NADPH oxidase in skeletal muscle sarcolemma has been proposed (32, 33). In addition, skeletal muscle contains NOX protein subunits and generates superoxide anion from NADH oxidation (30). However, neither the precise cellular location of this NOX activity nor its potential functional effects have been reported. Mitochondrial complexes I and III and cytoplasmic xanthine oxidase are major sources of superoxide anion in skeletal muscle (58, 59). Following muscle contraction, superoxide anion has been detected in the extracellular space (58, 60, 61). This free radical, which is not likely to diffuse as such through cell membranes, may undergo *in vivo* enzymatic or nonenzymatic dismutation to H_2O_2, a readily permeable and rather mild physiological oxidizing molecule (14) that targets reactive cysteine residues in cellular proteins (48). In muscle, H_2O_2 may readily react with the highly redox-sensitive RyR1, which is *S*-glutathionylated by H_2O_2 *in vitro* in the presence of GSH (62). The RyR1 isoform (63) is essential for skeletal muscle excitation-contraction (E-C) coupling, a process that requires close physical interactions between the RyR1 present in junctional SR and the DHPR, which acts as the voltage sensor protein of T-tubules responsible for RyR1 activation during E-C coupling (64). Skeletal RyR1 channels have a few cysteine residues highly responsive to oxidative modification at physiological pH (65), a property that makes them likely candi-
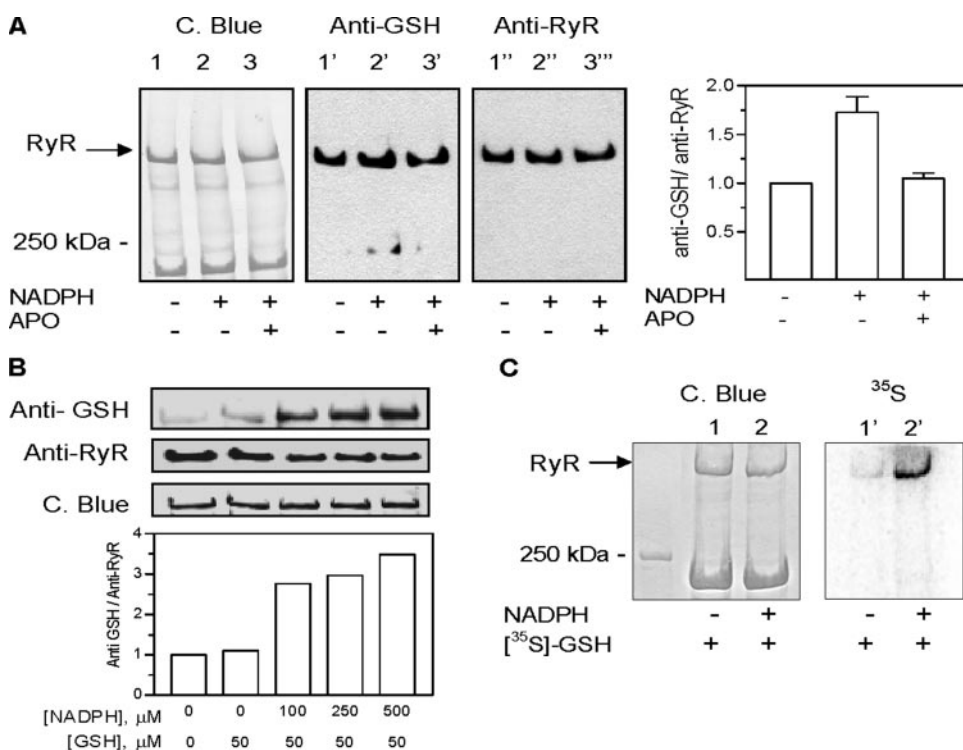
FIGURE 7. **Stimulation of RyR1 *S*-glutathionylation in triad vesicles by NADPH.** *A*, the *left panel* shows a blot stained with Coomassie Blue or developed with anti-GSH or anti-RyR antibodies, respectively. The *right panel* illustrates the ratio of their corresponding band densities (anti-GSH/anti-RyR), determined in native vesicles and after the addition of 0.1 mM NADPH or 0.1 mM NADPH + 8 mM apocynin (*APO*). *B*, the *upper panel* shows a blot developed with anti-GSH or anti-RyR antibodies or stained with Coomassie Blue. Each *lane* corresponds to vesicles incubated with the combinations of GSH and NADPH shown in the *lower panel*, which illustrates their corresponding band density ratios (anti-GSH/anti-RyR). *C*, triads were incubated with [^{35}S]GSH, and incorporation of ^{35}S into the RyR1 band was analyzed after separation by SDS-PAGE. The *left panel* (*lanes 1* and *2*) represents a gel stained with Coomassie Blue, and the *right panel* (*lanes 1'* and *2'*) corresponds to the ^{35}S radioactivity of the same gel, determined as detailed under "Experimental Procedures." *Lanes 1* and *1'*, control vesicles; *lanes 2* and *2'*, vesicles incubated with 0.1 mM NADPH.

dates to act as intracellular redox sensors (66, 67). *In vitro* experiments indicate that oxidation/alkylation, *S*-nitrosylation (38, 68), or *S*-glutathionylation (38, 62) of RyR1 hyperreactive SH residues enhances channel activity, whereas reduction to their free sulfhydryl state has the opposite effect (67–72). In particular, incubation of isolated SR vesicles with superoxide anion or H_2O_2 promotes RyR activation (42, 73–75).

Localization of the Skeletal Muscle NOX—The main goals of this work were 2-fold: to investigate the membrane origin of the skeletal muscle NOX activity and to study the potential effects of NOX-generated ROS on the highly redox-sensitive RyR1 channels. To address the first aim, we investigated the location of NOX components in intact muscle or in isolated vesicular preparations enriched in T-tubules, triads, or junctional (heavy) SR. The present results indicate that both gp91^{phox} and p47^{phox} colocalize with the α_{1s} DHPR subunit in T-tubules in adult muscle fibers. The two NOX2 integral membrane components (which form cytochrome b_{558}) were markedly enriched in isolated T-tubule vesicles; they were also present in triads but were completely absent from heavy SR vesicles. In addition, isolated triads displayed NADPH oxidative activity and had the capacity to generate both superoxide anion and H_2O_2 at the expense of NADPH oxidation.

Functional Effects of NOX Activity—We measured three different parameters of possible NOX-induced oxidative changes:

overall decrease in triadic free SH content, stimulation of RyR1 activity, and increase in RyR1 *S*-glutathionylation. We found that 0.1 mM NADH induced a significant decrease in the total sulfhydryl content of triads. This decrease was prevented by preincubation of triads with catalase, suggesting a direct role for H_2O_2 in this effect. The complete inhibition of SH oxidation produced by apocynin suggests that this reaction is due primarily to ROS generated by the T-tubular NOX.

Incubation of isolated SR vesicles with H_2O_2 increases RyR1 channel activity (42) and promotes RyR1 *S*-glutathionylation (62). Therefore, RyR1 are potential downstream targets of H_2O_2, a ROS product generated by the triad-associated NOX. The present results confirm this hypothesis. Incubation of triads with 0.1 mM NADPH or NADH increased [^{3}H]ryanodine binding rates, a widely accepted parameter of increased RyR activity. DPI inhibited the stimulation of [^{3}H]ryanodine binding rates produced by 0.1 mM NADPH, indicating NOX involvement in this activation. As expected from RyR1 channels modified by *S*-glutathionylation (38), both NADPH and H_2O_2 stimulated CICR kinetics in the presence of inhibitory Mg^{2+} concentrations. These results suggest strongly that the triad-associated NOX can activate RyR1-mediated CICR.

It has been reported that skeletal muscle SR contains a DPI-insensitive NADH-dependent oxidase activity that reduces molecular oxygen to generate superoxide and that co-purifies with RyR1 (43); this report also showed that the addition of 1 mM NADH enhanced 2.2-fold the rates of [^{3}H]ryanodine binding to SR vesicles, whereas 1 mM NADPH was less effective. However, the lack of DPI inhibition and the lower activity obtained with NADPH than NADH make unlikely NOX participation in these reported effects. We found that 1 mM NADH stimulated [^{3}H]ryanodine binding to triads twice as much as 0.1 mM NADH; furthermore, and as reported (43), DPI did not decrease this stimulation. These results suggest that the T-tubule NOX is not involved in the activation of RyR1 channels produced by 1 mM NADH.

Physiological Implications—In summary, our work shows that the skeletal muscle T-tubules possess a functional nonphagocytic NOX activity. This enzyme generates ROS, which in isolated triads decrease the total sulfhydryl content and activate RyR1 through *S*-glutathionylation, a specific cysteine redox modification that enhances calcium release mediated by RyR1 (38) or RyR2 (29). We propose that in intact muscle fibers, RyR1

channels, which are essential components of the E-C coupling molecular machinery, are downstream targets of this T-tubule NOX activity. As a result of NOX-induced *S*-glutathionylation, RyR1 channels would increase their activity, producing increased CICR even in the presence of the high intracellular Mg^{2+} concentrations present in intact fibers (38). Our recent findings using field stimulation at tetanic frequencies of rat skeletal muscle myotubes in primary culture support this proposal. Thus, we have found that tetanic stimulation elicits significant ROS generation and produces large ryanodine-sensitive intracellular Ca^{2+} signals and that DPI addition significantly reduces both responses.[4] These results suggest that tetanic stimulation of muscle enhances RyR-mediated calcium release via NOX-generated ROS.

However, a definitive demonstration of the relevance of RyR1 redox modification in the context of physiological gating of the channel during E-C coupling is missing. Following contraction, skeletal muscle fibers appear to release significant amounts of superoxide anion together with nitric oxide into the external medium (56, 57, 76, 77). However, in skinned muscle fibers, exogenous H_2O_2 stimulates contractions induced by caffeine but not by action potentials (78). Furthermore, H_2O_2 activates contraction in intact skeletal muscle fibers without an apparent increase in cytoplasmic Ca^{2+} concentration (79) despite the fact that, as shown here, H_2O_2 readily activates RyR1-mediated calcium release (see also Ref. 42). These apparently contradictory results can be reconciled by assuming that exogenous H_2O_2 is readily scavenged by the skeletal muscle antioxidant defense systems (*i.e.* catalase or glutathione) before reaching RyR1 at the triads. This proposal highlights the relevance of the ROS source location, since *in situ* NOX-mediated generation of superoxide anion and H_2O_2 at the T-tubules may escape the scavenging effects of endogenous antioxidant systems, allowing RyR1 modification in the highly restricted triadic space. As discussed above, tetanic stimulation enhances RyR1-mediated calcium release in muscle cells in primary culture via NOX-generated ROS.[4] In addition, preliminary results[6] indicate that K^+-induced depolarization of C2C12 cells enhances NOX-dependent RyR1 *S*-glutathionylation. Hence, the privileged location of the skeletal muscle NOX at the T-tubules and its activation by strong depolarization open the possibility that conditions of increased muscle activity, such as exercise, stimulate Ca^{2+} release through NOX-induced RyR1 redox activation. It remains to be determined, however, if NOX-generated ROS modulate E-C coupling in intact muscle fibers.

REFERENCES

1. Lambeth, J. D. (2004) *Nat. Rev. Immunol.* **4,** 181–189
2. Vignais, P. V. (2002) *Cell Mol. Life Sci.* **59,** 1428–1459
3. Quinn, M. T., and Gauss, K. A. (2004) *J. Leukocyte Biol.* **76,** 760–781
4. Babior, B. M. (2000) *Am. J. Med.* **109,** 33–44
5. Jones, S. A., O'Donnell, V. B., Wood, J. D., Broughton, J. P., Hughes, E. J., and Jones, O. T. (1996) *Am. J. Physiol.* **271,** H1626–H1634
6. Bayraktutan, U., Draper, N., Lang, D., and Shah, A. M. (1998) *Cardiovasc. Res.* **38,** 256–262
7. Noh, K. M., and Koh, J. Y. (2000) *J. Neurosci.* **20,** RC111
8. Tammariello, S. P., Quinn, M. T., and Estus, S. (2000) *J. Neurosci.* **20,** RC53
9. Tejada-Simon, M. V., Serrano, F., Villasana, L. E., Kanterewicz, B. I., Wu, G. Y., Quinn, M. T., and Klann, E. (2005) *Mol. Cell Neurosci.* **29,** 97–106
10. Bal-Price, A., Matthias, A., and Brown, G. C. (2002) *J. Neurochem.* **80,** 73–80
11. Geiszt, M., and Leto, T. L. (2004) *J. Biol. Chem.* **279,** 51715–51718
12. Griendling, K. K. (2004) *Heart* **90,** 491–493
13. Thannickal, V. J., and Fanburg, B. L. (1995) *J. Biol. Chem.* **270,** 30334–30338
14. Rhee, S. G., Bae, Y. S., Lee, S. R., and Kwon, J. (2000) *Sci. STKE 2000,* E1
15. Ushio-Fukai, M., Zafari, A. M., Fukui, T., Ishizaka, N., and Griendling, K. K. (1996) *J. Biol. Chem.* **271,** 23317–23321
16. Krieger-Brauer, H. I., Medda, P. K., and Kather, H. (1997) *J. Biol. Chem.* **272,** 10135–10143
17. Mahadev, K., Wu, X., Zilbering, A., Zhu, L., Lawrence, J. T., and Goldstein, B. J. (2001) *J. Biol. Chem.* **276,** 48662–48669
18. DeCoursey, T. E., Morgan, D., and Cherny, V. V. (2003) *Nature* **422,** 531–534
19. Sohn, H. Y., Keller, M., Gloe, T., Morawietz, H., Rueckschloss, U., and Pohl, U. (2000) *J. Biol. Chem.* **275,** 18745–18750
20. Matsuzaki, I., Chatterjee, S., Debolt, K., Manevich, Y., Zhang, Q., and Fisher, A. B. (2005) *Am. J. Physiol.* **288,** H336–H343
21. Kishida, K. T., Pao, M., Holland, S. M., and Klann, E. (2005) *J. Neurochem.* **94,** 299–306
22. Bokoch, G. M., and Diebold, B. A. (2002) *Blood* **100,** 2692–2696
23. Martyn, K. D., Frederick, L. M., von Loehneysen, K., Dinauer, M. C., and Knaus, U. G. (2006) *Cell. Signal.* **18,** 69–82
24. Banfi, B., Tirone, F., Durussel, I., Knisz, J., Moskwa, P., Molnar, G. Z., Krause, K. H., and Cox, J. A. (2004) *J. Biol. Chem.* **279,** 18583–18591
25. Banfi, B., Clark, R. A., Steger, K., and Krause, K. H. (2003) *J. Biol. Chem.* **278,** 3510–3513
26. Takeya, R., Ueno, N., Kami, K., Taura, M., Kohjima, M., Izaki, T., Nunoi, H., and Sumimoto, H. (2003) *J. Biol. Chem.* **278,** 25234–25246
27. Cheng, G., Ritsick, D., and Lambeth, J. D. (2004) *J. Biol. Chem.* **279,** 34250–34255
28. Byrne, J. A., Grieve, D. J., Bendall, J. K., Li, J. M., Gove, C., Lambeth, J. D., Cave, A. C., and Shah, A. M. (2003) *Circ. Res.* **93,** 802–805
29. Sánchez, G., Pedrozo, Z., Domenech, R. J., Hidalgo, C., and Donoso, P. (2005) *J. Mol. Cell Cardiol.* **39,** 982–991
30. Javesghani, D., Magder, S. A., Barreiro, E., Quinn, M. T., and Hussain, S. N. (2002) *Am. J. Respir. Crit. Care Med.* **165,** 412–418
31. Cheng, G., Cao, Z., Xu, X., van Meir, E. G., and Lambeth, J. D. (2001) *Gene (Amst.)* **269,** 131–140
32. Brotto, M. A., and Nosek, T. M. (1996) *J. Appl. Physiol.* **81,** 731–737
33. Reid, M. B. (2001) *J. Appl. Physiol.* **90,** 724–731
34. Burritt, J. B., Quinn, M. T., Jutila, M. A., Bond, C. W., and Jesaitis, A. J. (1995) *J. Biol. Chem.* **270,** 16974–16980
35. Hidalgo, C., González, M. E., and Lagos, R. (1983) *J. Biol. Chem.* **259,** 13937–13945
36. Hidalgo, C., Jorquera, J., Tapia, V., and Donoso, P. (1993) *J. Biol. Chem.* **268,** 15111–15117
37. Hartree, E. F. (1972) *Anal. Biochem.* **48,** 422–427
38. Aracena, P., Sanchez, G., Donoso, P., Hamilton, S. L., and Hidalgo, C. (2003) *J. Biol. Chem.* **278,** 42927–42935
39. Zhou, M., Diwu, Z., Panchuk-Voloshina, N., and Haugland, R. P. (1997) *Anal. Biochem.* **253,** 162–168
40. Ellman, G. L. (1959) *Arch. Biochem. Biophys.* **82,** 70–77
41. Aghdasi, B., Zhang, J. Z., Wu, Y., Reid, M. B., and Hamilton, S. L. (1997) *J. Biol. Chem.* **272,** 3739–3748
42. Favero, T. G., Zable, A. C., and Abramson, J. J. (1995) *J. Biol. Chem.* **270,** 25557–25563

43. Xia, R., Webb, J. A., Gnall, L. L., Cutler, K., and Abramson, J. J. (2003) *Am. J. Physiol.* **285,** C215–C221
44. Finkel, T. (1998) *Curr. Opin. Cell Biol.* **10,** 248–253
45. Thannickal, V. J., and Fanburg, B. L. (2000) *Am. J. Physiol.* **279,** L1005–L1028
46. Bae, Y. S., Kang, S. W., Seo, M. S., Baines, I. C., Tekle, E., Chock, P. B., and Rhee, S. G. (1997) *J. Biol. Chem.* **272,** 217–221
47. Droge, W. (2002) *Physiol. Rev.* **82,** 47–95
48. Rhee, S. G., Chang, T. S., Bae, Y. S., Lee, S. R., and Kang, S. W. (2003) *J. Am. Soc. Nephrol.* **14,** S211–S215
49. Aslund, F., Zheng, M., Beckwith, J., and Storz, G. (1999) *Proc. Natl. Acad. Sci. U. S. A.* **96,** 6161–6165
50. Marshall, H. E., Merchant, K., and Stamler, J. S. (2000) *FASEB J.* **14,** 1889–1900
51. Martindale, J. L., and Holbrook, N. J. (2002) *J. Cell Physiol.* **192,** 1–15
52. Fernandes, A. P., and Holmgren, A. (2004) *Antioxid. Redox. Signal.* **6,** 63–74
53. Shelton, M. D., Chock, P. B., and Mieyal, J. J. (2005) *Antioxid. Redox. Signal.* **7,** 348–366
54. Haugaard, N. (2000) *Ann. N. Y. Acad. Sci.* **899,** 148–158
55. Cooper, C. E., Patel, R. P., Brookes, P. S., and Darley-Usmar, V. M. (2002) *Trends Biochem. Sci.* **27,** 489–492
56. Bejma, J., and Ji, L. L. (1999) *J. Appl. Physiol.* **87,** 465–470
57. Reid, M. B., and Durham, W. J. (2002) *Ann. N. Y. Acad. Sci.* **959,** 108–116
58. Stofan, D. A., Callahan, L. A., DiMarco, A. F., Nethery, D. E., and Supinski, G. S. (2000) *Am. J. Respir. Crit. Care Med.* **161,** 891–898
59. Nethery, D., Stofan, D., Callahan, L., Dimarco, A., and Supinski, G. (1999) *J. Appl. Physiol.* **87,** 792–800
60. Reid, M. B., Shoji, T., Moody, M. R., and Entman, M. L. (1992) *J. Appl. Physiol.* **73,** 1805–1809
61. Zuo, L., Christofi, F. L., Wright, V. P., Liu, C. Y., Merola, A. J., Berliner, L. J., and Clanton, T. L. (2000) *Am. J. Physiol.* **279,** C1058–C1066
62. Aracena, P., Tang, W., Hamilton, S. L., and Hidalgo, C. (2005) *Antioxid. Redox. Signal.* **7,** 870–881
63. Fill, M., and Copello, J. A. (2002) *Physiol. Rev.* **82,** 893–922
64. Ríos, E., and Pizarro, G. (1991) *Physiol. Rev.* **71,** 849–908
65. Pessah, I. N. (2001) *Pest. Manag. Sci.* **57,** 941–945
66. Pessah, I. N., Kim, K. H., and Feng, W. (2002) *Front. Biosci.* **7,** a72–a79
67. Hidalgo, C., Donoso, P., and Carrasco, M. A. (2005) *IUBMB Life* **57,** 315–322
68. Sun, J., Xu, L., Eu, J. P., Stamler, J. S., and Meissner, G. (2001) *J. Biol. Chem.* **276,** 15625–15630
69. Zable, A. C., Favero, T. G., and Abramson, J. J. (1997) *J. Biol. Chem.* **272,** 7069–7077
70. Marengo, J. J., Hidalgo, C., and Bull, R. (1998) *Biophys. J.* **74,** 1263–1277
71. Feng, W., Liu, G., Allen, P. D., and Pessah, I. N. (2000) *J. Biol. Chem.* **275,** 35902–35907
72. Oba, T., Murayama, T., and Ogawa, Y. (2002) *Am. J. Physiol.* **282,** C684–C692
73. Suzuki, Y. J., Cleemann, L., Abernethy, D. R., and Morad, M. (1998) *Free Radic. Biol. Med.* **24,** 318–325
74. Kawakami, M., and Okabe, E. (1998) *Mol. Pharmacol.* **53,** 497–503
75. Oba, T., Ishikawa, T., Murayama, T., Ogawa, Y., and Yamaguchi, M. (2000) *Am. J. Physiol.* **279,** C1366–C1374
76. Grozdanovic, Z. (2001) *Microsc. Res. Tech.* **55,** 148–153
77. Jackson, M. J. (2005) *Philos. Trans. R. Soc. Lond. B Biol. Sci.* **360,** 2285–2291
78. Posterino, G. S., Cellini, M. A., and Lamb, G. D. (2003) *J. Physiol.* **547,** 807–823
79. Andrade, F. H., Reid, M. B., Allen, D. G., and Westerblad, H. (1998) *J. Physiol.* **509,** 565–575